

# Effects of Texture on the Electrochemical Properties of Single Grains in Polycrystalline Zinc

Chan-Jin Park, Manuel M. Lohrengel\*, Tobias Hamelmann\*,  
Milan Pilaski\*, and Hyuk-Sang Kwon

*Dept. of Materials Science and Engineering, Korea Advanced Institute of Science and Technology  
373-1, Kusong-dong, Yusong-gu, Taejon 305-701, South Korea*

*\*Institute for Physical Chemistry and Electrochemistry, Heinrich-Heine-University  
Duesseldorf, Duesseldorf 40225, Germany*

Effects of texture on the electrochemical behaviors of single grains in polycrystalline zinc were investigated using a capillary-based micro-droplet cell. Potentiodynamic sweeps and capacity measurements were carried out in pH 9 borate buffer solution. The cyclic voltammograms and the capacity measurements on single grains with different crystallographic orientations in polycrystalline Zn showed a strong dependence of oxide growth on crystallographic grain orientation. The total charge consumed for oxide formation and the inverse capacity increased with an increase of surface packing density of grain, suggesting the oxide formation was greater on grains with higher surface packing density.

**Keywords** : zinc, micro-droplet cell, texture, cyclic voltammogram, capacity, oxide growth

## 1. Introduction

Characterization of passive film on a metal surface is traditionally in the domain of electrochemical methods. Because of the low lateral resolution of electrochemical standards methods, however, only macroscopic averaged properties could be obtained. Therefore, important texture depending characteristics on polycrystalline material were rarely investigated. Except for single crystals, which are specially controlled during solidification, most metals consist of many grains with various crystallographic orientations. Thus, the macroscopic electrochemical behavior is simply the sum of the contributions of the different grains, multiplied by their individual degree of coverage. Sometimes, some special grains showing completely different properties compared with others may dominate the electrochemical response of a macroscopic sample.

A new electrochemical device, the capillary-based droplet cell<sup>1)</sup> shown in Fig. 1, gives facilities for micro-electrochemical investigation at high resolution. The wetted area defines the working electrode, and the reference and counter electrodes are combined with a capillary with a tip diameter of 20 ~ 600  $\mu\text{m}$ . The small area of the working electrode determined by the tip size of the capillary enables measurement of the electrochemical signals of small areas within a single grain. In addition,

this device has a smaller resolution than some special probe techniques (e.g. STM), but enables a complete range

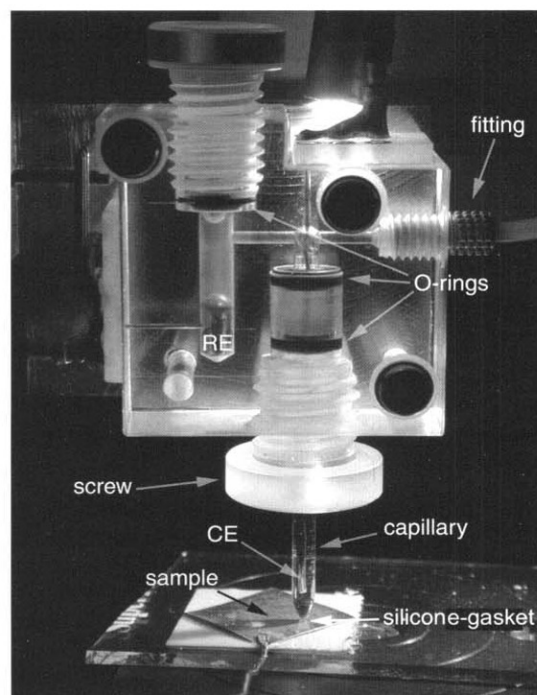


Fig. 1. Typical experimental setup of the micro-droplet cell.

of potentiostatic (or –dynamic) and galvanostatic (or –dynamic) techniques, including impedance spectroscopy. The method has already been applied to the single grains of polycrystalline materials such as steel, Al, Ta, Nb, and Hf,<sup>2)</sup> and some evidence of texture-depending characteristic of grains was found in those materials.

A few studies<sup>3),4)</sup> on the effect of crystallographic orientation on corrosion resistance of Zn were previously reported. However, in those studies single crystals or electrogalvanized coatings with well-defined surface orientation, e.g. (0001), (1010) and (1120), were used. Thus, measurement on surfaces with various crystal orientations was restricted. In addition, the test area was much larger compared with the size of real grains, even though area compensation was performed. Above all, in the previous works, little effort has been devoted to investigating the influence of crystallographic orientation on passivity of Zn.

The objective of the present study is to investigate systematically the effects of texture (crystallographic grain orientation) on the electrochemical behaviors of single grains in polycrystalline Zn using the droplet cell.

## 2. Experimental

The specimen used in the present study was prepared as a disk type with 10 mm diameter from a polycrystalline Zn (99.9999 %) rod, and annealed in an oven for 4 h at 280 °C to eliminate crystal defects and to increase the grain size to be suitable for investigation. The specimen was then mechanically polished up to 1 μm surface finish, and finally electropolished in 10 % (vol.) HClO<sub>4</sub> + 90 % CH<sub>3</sub>COOH solution.

Potentiodynamic sweeps and capacity measurements were carried out in a pH 9 borate buffer solution using the micro-droplet cell shown in Fig. 1. A capillary with an inner diameter of 37 μm (area:  $4.34 \times 10^{-5}$  cm<sup>2</sup>) was used for the measurement. After each experiment, the capillary was lifted and rinsed before a new position for measurement was addressed.

After the electrochemical experiments, the crystallographic orientation of the grains where the measurements were performed was determined by electron back scattering diffraction (EBSD) method. Two important crystallographic angles,  $\phi_1$  and  $\phi_2$ , were defined as shown in Fig. 2.  $\phi_1$  ranges from 0 to 90°, and  $\phi_2$  ranges from 0 to 30° since the hexagonal closed packed (hcp) structure has a D<sub>6h</sub> symmetry, which includes a six-fold rotation and a perpendicular mirror plane. For instance, the basal (0001) plane has the values of  $\phi_1 = 0^\circ$  and  $\phi_2 = 0 \sim 30^\circ$ ; for (0110),  $\phi_1 = 90^\circ$  and  $\phi_2 = 30^\circ$ ; and for (1120),  $\phi_1 = 90^\circ$ ,  $\phi_2 =$

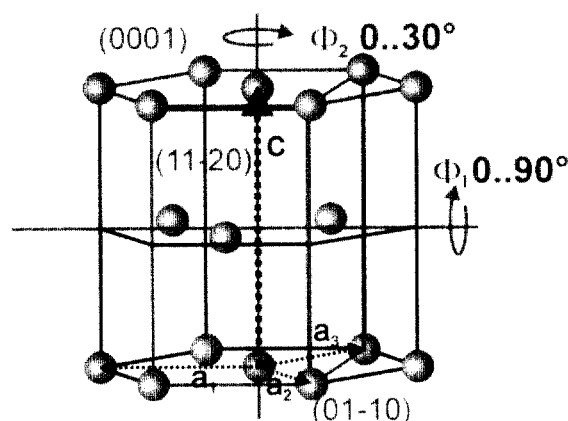


Fig. 2. Typical hexagonal close packed structure and rotation axis  $\phi_1$  and  $\phi_2$  for the determination of crystallographic grain orientation.

0°. The (0110) and (1120) planes have surface packing densities of 0.54 and 0.47 relative to the basal plane. Generally, as  $\phi_1$  is closer to 0°, the grains have high packing density closer to that of the basal (0001) plane.

## 3. Results

Fig. 3 shows the microstructure of pure Zn, which was electropolished in 10 % HClO<sub>4</sub> + 90 % CH<sub>3</sub>COOH solution. The small circles indicate the points where the electrochemical tests were conducted using the micro-droplet cell. Each grain is easily distinguished by its color, which ranges from navy blue to white. The different color of each grain is probably due to the different electronic characteristics of the outer film, which was formed during the electropolishing. In addition, the film characteristics may be associated with the grain orientation of its substrate.

For the positions indicated as small circles in Fig. 3, the potentials sweeps and capacity measurements were carried out in a pH 9 borate buffer solution, and the results are shown in Fig. 4. In addition, the crystallographic grain orientations of each grain were determined. The results showed strong dependence of cyclic voltammograms and capacity curves on the crystallographic grain orientation. Grains (a) and (b) with  $\phi_1 = 23^\circ$ ,  $\phi_2 = 28^\circ$  and  $\phi_1 = 58^\circ$ ,  $\phi_2 = 9^\circ$ , respectively, showed larger activation peaks and reached plateau current more slowly than other grains. Especially, the capacity of grain (a), which had the highest surface packing density, was much smaller than those of the others.

Several important electrochemical parameters such as the plateau current density ( $i_{\text{plat}}$ ) and the total charge ( $Q_{\text{tot}}$ ) were determined from Fig. 4, and are shown in Table 1.

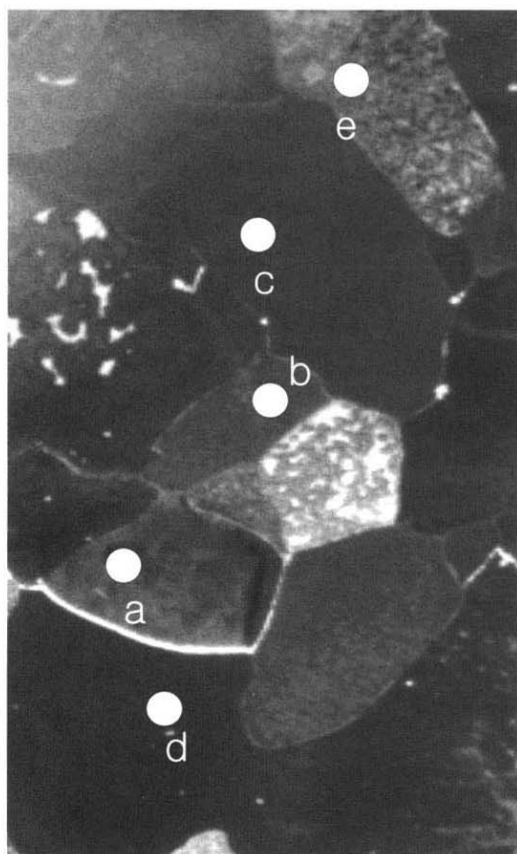


**Fig. 3.** Microstructure of pure Zn, which was electropolished in 10 % HClO<sub>4</sub> + 90 % CH<sub>3</sub>COOH solution. The small circles indicate the points where the electrochemical tests were performed.

The plateau current density ( $I_{\text{plat}}$ ) was largest for grain (d) with  $\phi_1 = 69^\circ$ ,  $\phi_2 = 29^\circ$ , and seemed to correlate better with  $\phi_2$  than  $\phi_1$ ; the  $I_{\text{plat}}$  increased with an increase of  $\phi_2$  (Table 1, Fig. 5). The large  $I_{\text{plat}}$  indicates small electric field strength ( $E_{\text{ox}}$ ) in the oxide film and high ionic mobility. However, the  $I_{\text{plats}}$  of each grain, except that of

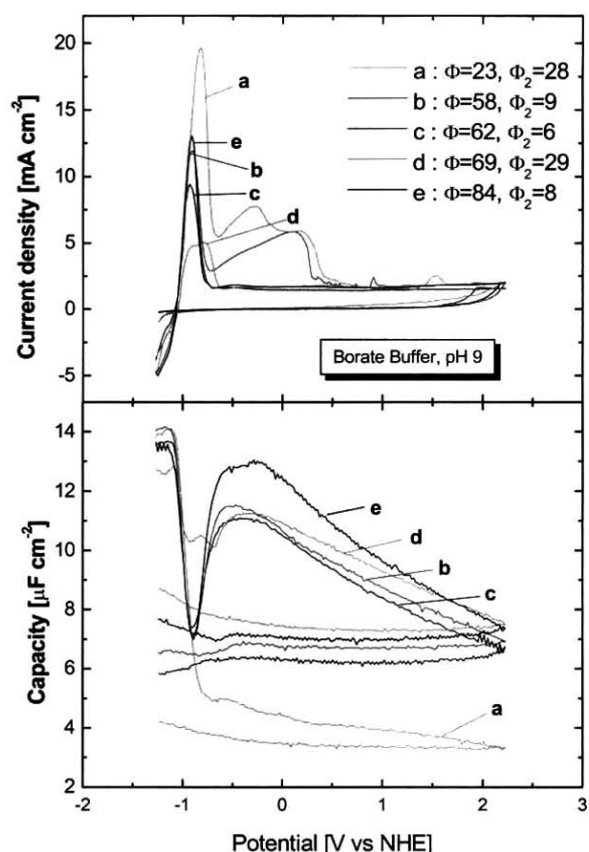


**Fig. 4.** Potential-current curves and corresponding capacities of different grains of Zn in pH 9, borate buffer solution.

grain (c), were similar to figure out the relation between the  $i_{\text{plat}}$  and the crystallographic angles. The total charge ( $Q_{\text{tot}}$ ) and the inverse minimum capacity ( $C_{\text{min}}^{-1}$ ) during anodic polarization showed better correlation with the crystallographic angles, especially with  $\phi_1$ , as can be seen in Fig. 5.  $Q_{\text{tot}}$  decreased with an increase of  $\phi_1$ , and  $C_{\text{min}}^{-1}$ , which is proportional to the film thickness, showed a similar tendency, reflecting that  $Q_{\text{tot}}$  is also closely

**Table 1. Summary of electrochemical parameters determined from the cyclic voltammograms and capacity measurements on different grains of polycrystalline Zn.**

Grain	$\phi_1$	$\phi_2$	$I_{\text{plat}}$ [mA/cm <sup>2</sup> ]	$I_{\text{peak}}$ [mA/cm <sup>2</sup> ]	$Q_{\text{tot}}$ [mC/cm <sup>2</sup> ]	$Q_{\text{peak}}$ [mC/cm <sup>2</sup> ]	$C_{\text{max}}$ [F/cm <sup>2</sup> ]	$C_{\text{min}}$ [F/cm <sup>2</sup> ]
a	23	28	1.82	19.6	140	45.0	5.0	3.33
b	58	9	1.90	11.9	106	23.0	11.5	6.93
c	62	6	1.51	9.4	61	17.4	11.1	6.54
d	69	29	1.95	5.0	66	16.5	11.2	7.50
e	84	8	1.90	13.0	73	22.5	13.0	7.46

\*  $I_{\text{plat}}$ : the plateau current;  $I_{\text{peak}}$ : the active dissolution peak current;  $Q_{\text{tot}}$ : the total charge,  $Q_{\text{peak}}$ : the dissolution peak charge;  $C_{\text{max}}$ : the maximum capacity;  $C_{\text{min}}$ : the minimum capacity

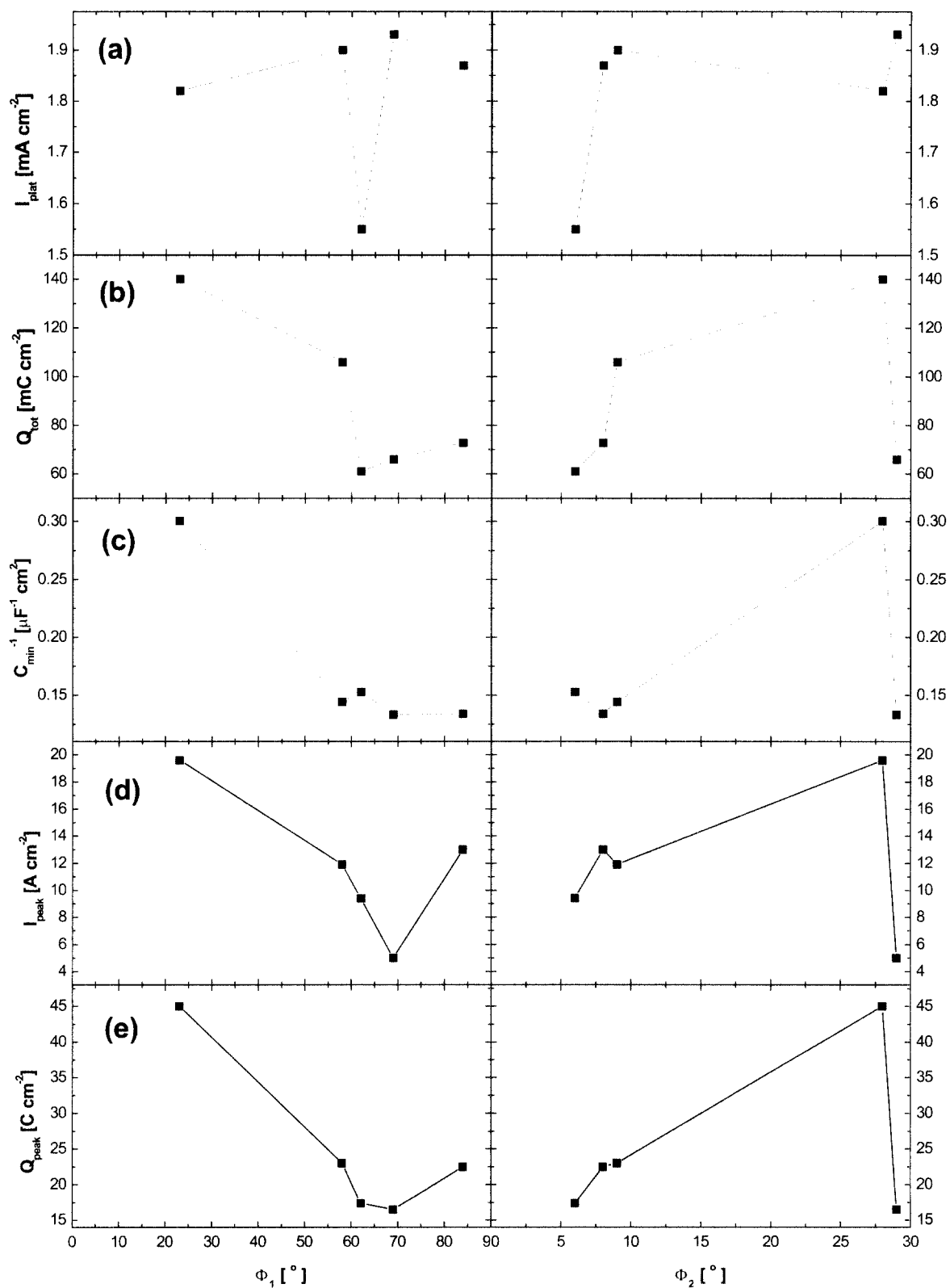


**Fig. 5.** The plateau current (a), the total charge (b), the inverse minimum capacity (c), the peak current (c), and the peak charge (d) on different grains of polycrystalline Zn as a function of  $\phi_1$  and  $\phi_2$ .

associated with the  $C_{\min}^{-1}$ .

This suggests that all charges (peak + plateau) were consumed for layer formation, assuming the grain independent dielectric constant (for polycrystalline zinc,  $\epsilon = 8.5^{5,6}$ ) and excluding notable active dissolution without precipitation. Popova, Bagotskii, and Kabanov<sup>7</sup> suggested the total charges for passivation  $Q_p = Q_1 + Q_2$ , where the quantity  $Q_1$  relates to zinc dissolution and to diffusion-related concentration charges at the electrode-solution interface, and the quantity  $Q_2$  relates to the charges in surface state leading to passivation, e.g., film formation. In most media the amount of charge directly leading to passivity corresponds to the equivalent of about a monomolecular layer of oxygen or zinc oxide.<sup>7</sup>

From the results, the oxide formation seems to be greater on grains with lower  $\phi_1$ . In contrast, the current density of the anodic dissolution peak ( $I_{\text{peak}}$ ) and its charge consumed ( $Q_{\text{peak}}$ ) didn't correlate with the crystallographic angles as highly as the total charge and the inverse capacity did. This is presumably due to the different initial surface conditions (e.g. surface roughness, former film characteristics) after the electropolishing. It has been reported that at the onset of electropolishing, a gray coating covered the surface of Zn, and the film had the same character as the passive film.<sup>8</sup> In addition, this solid film, in close contact with the metal surface, suppressed etching by insuring formation of random vacancies at the zinc-film interface.<sup>8</sup> The formation of gray-colored film during the electropolishing was also confirmed in the present work. Thus, the prior film formation on the surface seemed to affect the active dissolution of each grain despite that the surface was cleaned for several minutes in an ultrasonic bath after the electropolishing. In addition, this film might affect the further passivation procedure. However, the oxide film formed during following anodic polarization dominates the electrochemical responses of the sample before long with the film growth.

#### 4. Discussion

Results of the present work showed strong dependence of the cyclic voltammograms and capacities on the crystallographic grain orientation. In conclusion, oxide formation was greater on low index grains compared with high index

ones. The strong correlation between crystallographic grain orientation and oxide growth indicates the formation of a crystalline oxide. Specifically, the growth may take place at the metal/film interface inducing the strong dependence on the crystallographic surface structure of this interface. Some evidence<sup>9</sup> of hexagonal cell structure of oxide film with a cell size of about 3000 Å was reported in a previous study. However, the mechanism whereby zinc is oxidized still remains in doubt, and it should be elucidated in future study.

#### 5. Conclusion

The cyclic voltammograms and the capacity measurements on single grains with different crystallographic orientations in polycrystalline Zn showed a strong dependence of oxide growth on crystallographic grain orientation. The total charge ( $Q_{\text{tot}}$ ) consumed for oxide formation and the inverse capacity ( $C_{\min}^{-1}$ ) increased with an increase of the  $\phi_1$ , suggesting the oxide formation was greater on grains with higher surface packing density.

#### References

1. M. M. Lohrengel, A. Moehring, and M. Pilaski, *J. Anal. Chem.* **367**, 334 (2000).
2. A. Moehring, and M. M. Lohrengel in "PASSIVITY OF METALS AND SEMICONDUCTORS" Proceedings of the 8<sup>th</sup> International Symposium, edited by A. B. Ives, J. L. Luo and J. Rodda, The Electrochemical Society, Pennington, New Jersey, PV **99-42**, 114 (2000).
3. R. F. Ashton, and M. T. Hepworth, *Corrosion*, **24**, 50 (1968).
4. H. Park and J. A. Szpunar, *Corrosion Science*, **40**, 525 (1998).
5. J. R. Vilche, K. Juttner, W. J. Lorenz, W. Kautek, W. Paatsch, M. H. Dean, and U. Stimming, *J. Electrochem. Soc.*, **136**, 3773 (1989).
6. N. Sato and K. Kudo, *Electrochim. Acta*, **16**, 447 (1971).
7. T. I. Popova, V. S. Bagotski, and B. N. Kabanov, *Dokl. Akad. Nauk SSSR*, **132**, 639 (1960).
8. A. J. Bard, "Encyclopedia of electrochemistry of the elements", Vol. 5, MARCEL DEKKER, INC., p.48. (1976).
9. H. Fry and M. Whitaker, *J. Electrochem. Soc.* **106**, 606 (1959).